

This is the accepted manuscript made available via CHORUS. The article has been published as:

Tuning coupling: Discrete changes in runaway avalanche sizes in disordered media

Braden A. W. Brinkman and Karin A. Dahmen

Phys. Rev. E **84**, 041129 — Published 19 October 2011

DOI: [10.1103/PhysRevE.84.041129](https://doi.org/10.1103/PhysRevE.84.041129)

Tuning Coupling: Discrete Changes in Runaway Avalanche Sizes in Disordered Media

Braden A. W. Brinkman and Karin A. Dahmen

*Department of Physics, University of Illinois at Urbana-Champaign,
1110 West Green Street Urbana, Illinois 61801-3080*

Hysteretic systems may exhibit a runaway avalanche in which a large fraction of the constituents of the system collectively change state. It would be very valuable to understand the role that interaction strength between constituents has on the size such catastrophic runaway avalanches. We use a simple model, the random field Ising model, to study how the size of the runaway avalanche changes as the coupling between spins, J , is tuned. In particular, we calculate $P(S)$, the distribution of size-changes, S , in the runaway avalanche size as J is towards a critical value J_c , and find that the distribution scales as $P(S) \sim S^{-\tau} \mathcal{D}(S^\sigma(J/J_c - 1))$, with τ and σ critical exponents and $\mathcal{D}(x)$ a universal scaling function. In mean field theory we find $\tau = 3/2$, $\sigma = 1/2$ and $\mathcal{D}(x) = \exp(-(3x)^{1/\sigma}/2)$. On the basis of these results and previous studies we also predict that for three dimensions, $\tau = 1.6$ and $\sigma = 0.24$.

PACS numbers: 75.60.Ej, 05.40.Ca, 75.10.Hk, 75.50.Lk

I. INTRODUCTION

Many systems driven out of equilibrium are hysteretic and exhibit avalanche dynamics as the driving field or force is changed.¹ Often there is a macroscopic runaway avalanche indicated by a discontinuous jump in the hysteresis curve of some measured quantity, such as magnetization in ferromagnetic systems. Other examples of such phenomena include fault slips in earthquakes and fluids invading porous media.¹ Because these runaway avalanches span the entire system, understanding how the coupling strength of interactions between constituents of the system affects the runaway avalanche size has important consequences of making more robust magnetic materials or memory storage devices, or preventing large failure avalanches, such as in power grids. Although such systems may have very different microscopic origins, the statistics of avalanches are often exactly the same. Many microscopic details become increasingly irrelevant when viewed at larger and larger length scales, a concept known as universality.¹ Due to universality, we may calculate the properties of these statistics in simple models and make predictions for more complicated real experimental systems.

To this end, we may study the effects that tuning the coupling strength have on runaway avalanches exhibited in a simple model. The random field Ising model (RFIM) is a simple model that captures the essential properties of avalanches in ferromagnetic materials. Due to universality and the fact the Ising model has been used to model many different systems, studying this model is a natural choice for understanding general properties of avalanches.^{2–19} The RFIM models a lattice of locally interacting magnetic spins, each subject to a different random local field, h_i , where i labels the site at which the random local field is applied. The avalanche statistics are controlled by the ratio J/R of the coupling between spins, J , to the disorder, R (measured by the standard deviation of the random local fields). The RFIM predicts that for J/R larger than some critical value, $(J/R)_c$, there

exists hysteresis with a discontinuous jump (runaway avalanche), ΔM , in the magnetization M as the external field H is varied. This is shown schematically in Fig. (1). The size of ΔM depends on $J/R - (J/R)_c$, the distance to the critical point, and vanishes at $J/R = (J/R)_c$. If an experimenter could tune J/R in a given sample, the runaway avalanche size ΔM , it would not vary smoothly as J/R is adjusted, but would instead change in discrete jumps. Understanding the statistics of these jumps could have important consequences for making more robust magnetic materials, memory storage devices or the prevention of large failure avalanches, such as in power grids.¹ In this paper we calculate the distribution of jump sizes in ΔM as J/R is tuned, which provides testable predictions for experiments.

To generate experimentally testable predictions we use the RFIM to calculate the distribution of the discrete jumps in the size of the runaway avalanche, ΔM , as the model parameter J/R is tuned. This calculation, done in a mean field approximation of the RFIM, will be a main result of this paper. In addition, results for the RFIM in three dimensions are extracted based on the connection of our results to previous studies of the RFIM,⁶ and we also consider the possibility of studying avalanches in materials with dipolar forces, which do not have runaway avalanches.

This paper is structured as follows: in section II we briefly review the RFIM, and describe avalanches in the model, with a focus on the mean field model. In section III we sketch the derivation of the distribution of jumps in the runaway avalanche size as J/R is tuned. In section IV we discuss numerical simulations performed to check our theoretical predictions. In section V we briefly discuss the three dimensional RFIM and we predict values for the critical exponents in three dimensions, and in section VI we briefly discuss avalanches in materials with dipolar forces, in which there are no runaway avalanches. In section VII we discuss possibilities for experimentally measuring the critical exponents discussed in the text, and in section VIII we summarize the work and discuss

future directions.

II. THE RANDOM FIELD ISING MODEL

The random field Ising model (RFIM) is a relatively simple model of interacting spins that has been used to study driven, disordered, non-equilibrium systems with hysteresis and avalanches.^{2–19} The model exhibits a second order phase transition as J/R is tuned. Above the critical ratio $(J/R)_c$ the magnetization of the system exhibits a runaway avalanche in which large numbers of spins collectively reverse orientation as an external longitudinal magnetic field H is swept from $-\infty$ to ∞ .^{2–6} The critical properties of the model near this transition will be universal for all models in the same universality class,¹ which is known to be quite large.³

The Hamiltonian for the RFIM is

$$\mathcal{H} = - \sum_{i,j} J_{ij} s_i s_j - \sum_{i=1}^N (H + h_i) s_i, \quad (1)$$

where the $s_i = \pm 1$ is the value of a classical spin located at site i . N is the total number of spins in the lattice, H is a global magnetic field parallel to the spin axis. The h_i are random magnetic fields, different at each site, drawn from a peaked distribution with width R . The parameter R characterizes the amount of disorder in the system. We choose a Gaussian distribution for simplicity:

$$\rho(h_i) = \frac{1}{\sqrt{2\pi}R} \exp \left[-\frac{h_i^2}{2R^2} \right]. \quad (2)$$

The scaling properties should remain the same for similarly shaped distributions.⁴

The factor J_{ij} is the interaction between spins i and j . For the standard RFIM in finite dimensions, J_{ij} couples only nearest neighbor spins. Such a model is generally difficult to solve analytically. Consequently, in this work we will focus on all-to-all (mean field) interactions, i.e., $J_{ij} = J/N$, all i, j , as mean field theory is often analytically tractable. The factor $1/N$ is required for the model to be well defined in the thermodynamic limit. In mean field theory, the Hamiltonian thus becomes

$$\mathcal{H}_{MF} = - \sum_{i=1}^N h_i^{MF,eff} s_i, \quad (3)$$

where each spin experiences an effective *local field*

$$h_i^{MF,eff} = JM + H + h_i. \quad (4)$$

The net magnetization M is given by

$$M = \frac{1}{N} \sum_{j=1}^N s_j, \quad (5)$$

and must be determined self consistently. At zero temperature, each spin aligns with its local effective field. Spins hence flip when the sign of their effective field changes. Due to the random fields h_i , the effective fields do not all change sign simultaneously, as in the case of zero disorder. Hence, as H is tuned it can trigger a single spin to flip, which will change M , which can in turn then cause further spins to flip, which may then cause more spins to flip, and so on until the cascade of spin flips peters out. These cascades of spin flips are avalanches that are detected as Barkhausen noise in experimental systems²⁰. In the thermodynamic limit, $N \rightarrow \infty$, and for $J > J_c$ there is an avalanche of size proportional to N in which a non-zero fraction of spins flips. This avalanche is referred to as the “runaway avalanche”. The fraction of spins flipped in all other avalanches is zero in the thermodynamic limit. They fall into two groups: avalanches which occur prior to the runaway avalanche are dubbed “precursors” and those which follow the runaway avalanche are termed “aftershocks”.

In mean field theory and in general, the runaway avalanche is detected experimentally as a discontinuous change, ΔM , in the magnetization as H is tuned. The size of the discontinuity depends on the coupling J . Fig. (2) shows the ΔM versus J curve which demonstrates a transition at $J = J_c$, where a runaway avalanche first appears and ΔM becomes non-zero. In the thermodynamic limit this curve is smooth. However, as shown in the figure, for finite N the curve has discrete jumps, which tend to zero as $N \rightarrow \infty$. These jumps in $\Delta M(J)$ are the central phenomenon that we study in this work: as J is tuned, the maximum avalanche size changes abruptly; the distribution of sizes of these changes is of interest as it has relevance to understanding - and potentially controlling - avalanches in many natural phenomena in systems such as power grids or magnetic materials.¹ Because the jumps in ΔM tend to zero in the thermodynamic limit, it is better to study jumps in the number of spins that flipped in the runaway avalanche, S_m , versus J instead. Jumps in the S_m versus J curve do not tend to zero as $N \rightarrow \infty$. S_m is related to ΔM by $\Delta M = 2S_m/N$. Determination of the distribution, $P(S)$, of jump sizes, S , in S_m will be the main result of this paper and a new prediction for experiments.

III. JUMP SIZE DISTRIBUTION DERIVATION

We begin our analysis by carefully considering what happens when a spin flips. We consider finite N first, taking the $N \rightarrow \infty$ limit in the end. Before the limit is taken, we identify the runaway avalanche as the largest avalanche, S_m , for $J \geq J_c$.

We initialize the system with $H = -\infty$. All spins initially point down as $h_i^{MF,eff}$ is dominated by H , and hence $M = -1$. The spins will flip in order of descending random fields, so we label the random fields $h_1 > h_2 > \dots > h_N$. The spin with random local field h_1 is the first

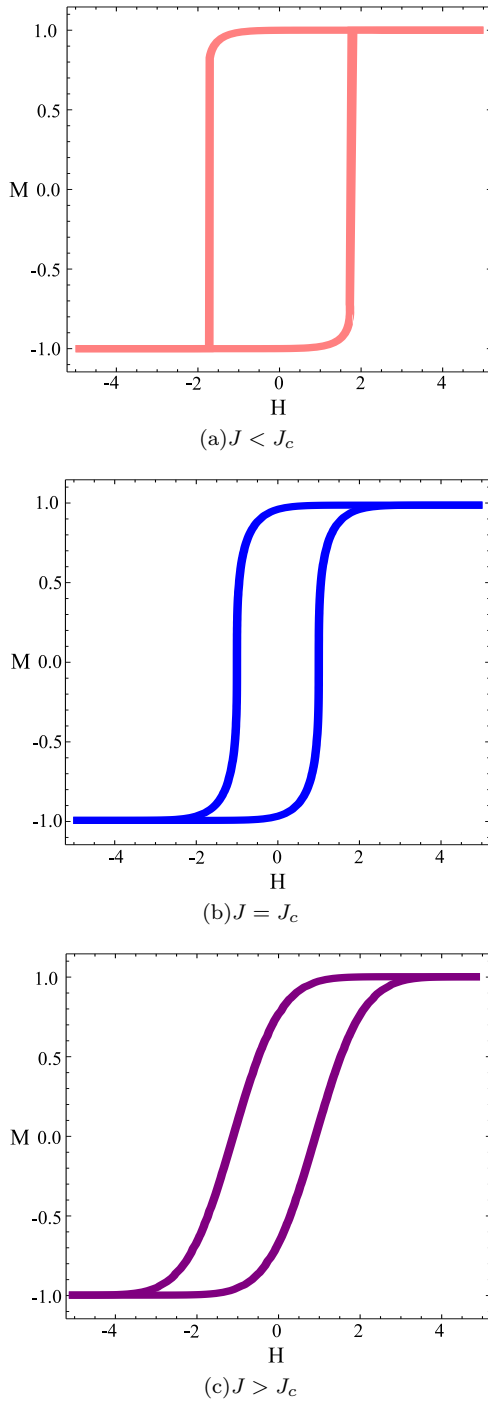


FIG. 1: (Color online) Plots of M versus H for the different coupling regimes. At $J = J_c$ the curve develops a discontinuity which grows with J . In mean field theory hysteresis only exists above J_c due to the simplicity of the hard spin model. The soft spin version of the mean field theory, however, displays hysteresis above and below J_c . It has the same critical exponents as the hard-spin mean field theory.⁴

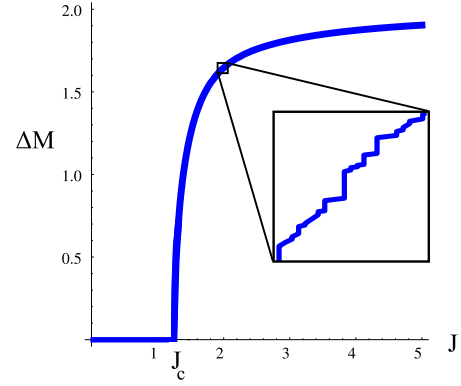


FIG. 2: (Color online) Plot of the size of the runaway avalanche, ΔM , vs. J . In the thermodynamic limit the curve appears smooth, but for finite N there are discrete jumps in the runaway avalanche size. We study jumps in $S_m = N\Delta M/2$, the total number of spins that flip in the runaway avalanche. The S_m vs. J curve will always have discrete jumps as N is increased, making it the appropriate curve to study.

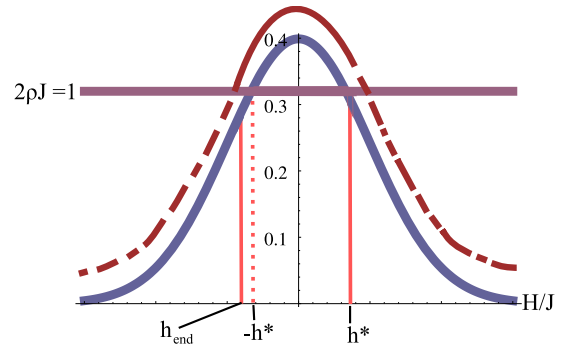


FIG. 3: (Color online) Schematic plot of avalanches in the RFIM system. The solid curve is a Gaussian distribution of random fields and the straight line indicates the line $2J\rho = 1$. The dashed line represents avalanches; each dash corresponds to an avalanche consisting of spins with random fields in the segment of the distribution below the dash. As H increases, spins with fields on the far right of the distribution begin to flip when the sign of their local field changes. The resulting avalanches peter out quickly as $n_{\text{flip}} = 2J\rho(h_0) \ll 1$. When the spin with local field h^* (Eq. 4) flips it triggers an avalanche for which $n_{\text{flip}} = 1$, enabling the avalanche to run away and cause a finite fraction of the spins to flip. As the avalanche travels to the left on the curve, eventually n_{flip} falls below 1 again once the spin with local field $-h^*$ has flipped, but due to the increase in effective field built up from spin flips during the runaway avalanche the system overshoots $-h^*$ and the avalanche peters out at some local field $|h| > |h^*|$. For J close to J_c , the overshoot is very slight, and the distribution of aftershock sizes close to $-h^*$ is given by Eq. (8).

spin to flip. When the longitudinal field H is tuned such that it causes a spin with field h_i to flip it increases the effective field of all other spins by $2J/N$. The condition that this spin flip causes the next spin, h_{i+1} , to flip is $h_i - h_{i+1} \leq 2J/N$. If spin i causes several spins to flip, then each flip will increase the effective field of all spins by $2J/N$, which can in turn flip even more spins. If n_i spins have flipped in the avalanche started by spin i , then the condition that the $(n_i + 1)^{\text{th}}$ spin flips is $h_i - h_{i+n_i} \leq 2Jn_i/N$. If the $(n_i + 1)^{\text{th}}$ spin does not flip, then there remains a “gap” between spins i and $i + n_i$, $\Delta_{i,i+n_i}$. This gap is given by $h_i - h_{i+n_i} = 2Jn_i/N + \Delta_{i,i+n_i}$, or

$$\Delta_{i,i+n_i}(J) = h_i - h_{i+n_i} - n_i \frac{2J}{N}. \quad (6)$$

The gap is a function of the coupling J . When $\Delta_{i,i+n_i}$ is positive the global field H must be increased to cause spin $i + n_i$ to flip. When $\Delta_{i,j}$ is negative, it means that spin j is already part of an avalanche caused by spin i . When $\Delta_{i,j} = 0$ spin i changes the effective field just enough to trigger spin j to flip. Thus, when studying changes in avalanche sizes as the coupling increases, we need only consider the gaps between pairs of spins for which $\Delta_{i,j}$ is positive, i.e., between the random fields of the initial spin of an avalanche and the initial spin of the avalanche that follows it. If we were to re-initialize the system with all spins pointing down, but with J adjusted so that the smallest positive $\Delta_{i,i+n_i}$ of the previous sweep of H vanishes, then when spin i flips, the resulting avalanche will now cause spin $i + n_i$ to flip. If spin i is the initial spin of an avalanche of size n_i with the smallest positive $\Delta_{i,i+n_i}$, then $J_{i,i+n_i}$, the value of J which will result in the avalanche flipping spin $i + n_i$, is given by

$$\frac{2J_{i,i+n_i}}{N} = \frac{h_i - h_{i+n_i}}{n_i}. \quad (7)$$

If during the previous sweep of H from $-\infty$ to $+\infty$ spin $i + n_i$, where n_i is the size of the avalanche started by spin i on the previous sweep, triggered an avalanche of size m_{i+n_i} , then spin i is now an avalanche of size $n_i + m_{i+n_i}$ on the current sweep (with coupling $J = J_{i,i+n_i}$). This is therefore how different avalanches join as J is increased. Because the gap $\Delta_{i,i+n_i}$ is now negative, for the next sweep we must look at the gap between spins i and $i + n_i + m_{i+n_i}$, $\Delta_{i,i+n_i+m_{i+n_i}}$, to determine if this gap or another one is the smallest gap on the current sweep of the system in order to determine what value to tune J to.

Although two avalanches have joined by increasing J , this has not necessarily caused a change in the runaway avalanche size S_m . To be precise, let $S_m^{(k)}$ denote the size of the largest avalanche on the k^{th} sweep of the system. We want to know which avalanche-joining processes will result in $S_m^{(k+1)} > S_m^{(k)}$ (as opposed to $S_m^{(k+1)} = S_m^{(k)}$). There are only three kinds of avalanche-joining processes which will increase S_m . The first pro-

cess we label “PP/AA”. In this process either two precursors have joined together or two aftershocks have joined together going from sweep k to sweep $k + 1$. In this case $S_m^{(k+1)} > S_m^{(k)}$ only if the sum of the two precursors/aftershocks that joined is greater than $S_m^{(k)}$. In the second process, labeled “PR”, spin i is the start of a precursor avalanche of size n_i and spin $i + n_i$ is the start of the runaway avalanche of size $S_m^{(k)}$. On the $(k + 1)^{\text{th}}$ sweep the size of the largest avalanche is then $S_m^{(k+1)} = S_m^{(k)} + n_i > S_m^{(k)}$. The largest avalanche size has thus increased. In the last process, labeled “RA”, spin i starts the largest avalanche of size $S_m^{(k)}$ and $i + S_m^{(k)}$ starts an aftershock, in which case $S_m^{(k+1)}$ is $S_m^{(k)} + n_{i+S_m^{(k)}} > S_m^{(k)}$ and the largest avalanche has increased between the k^{th} and $(k + 1)^{\text{th}}$ sweeps.

Above J_c and in the thermodynamic limit process RA dominates and processes PP/AA and PR are negligible. Process PP/AA is negligible because in the thermodynamic limit the ratio of largest avalanche size to the total number of spins, S_m/N , tends to a finite fraction $\Delta M/2$, whereas for a precursor/aftershock avalanche of size S , $S/N \rightarrow 0$ as $N \rightarrow \infty$. Thus, no two precursor/aftershock avalanches can ever join to become larger than the current S_m , and process PP/AA will not occur in the thermodynamic limit.

Process PR will not contribute in the thermodynamic limit because the gap between the runaway avalanche and the precursor avalanche preceding it will be larger than the gap between the runaway avalanche and the aftershock following it with probability 1 in the thermodynamic limit. The argument is as follows: Let $\Delta_{PR} = h_P - h_R - 2JS_P/N$ be the gap between the precursor to the runaway avalanche and the runaway avalanche, where h_P the field of the initial spin of the precursor avalanche, h_R the field at which the runaway avalanche starts and S_P the size of the precursor avalanche. Let $\Delta_{RA} = h_R - h_A - 2JS_m/N$ be the gap between the runaway avalanche and the aftershock following it, where h_A the field of the initial spin in the aftershock. On a given sweep of the system for which both gaps are positive, we want to know the values of J which will cause these gaps to vanish. The gap with the smaller coupling will vanish first as we increase J . However, because the fields are random, we can only calculate the probability $\Pr(0 < J_{PR} < J_{RA})$ that the coupling J_{RA} , which causes Δ_{RA} to vanish, is greater than the coupling J_{PR} , which causes Δ_{PR} to vanish. We show this probability is zero for arbitrary fields in the thermodynamic limit:

$$\begin{aligned}
& \Pr(0 < J_{PR} < J_{RA}) \\
&= \Pr\left(0 < \frac{2J_{PR}}{N} < \frac{2J_{RA}}{N}\right) \\
&= \Pr\left(0 < \frac{h_P - h_R}{S_P} < \frac{h_R - h_A}{S_m}\right) \\
&= \Pr\left(h_R < h_P < h_R + \frac{S_P}{S_m}(h_R - h_A)\right),
\end{aligned}$$

where in going to the third line we used the fact that $2J_{RA}/N = (h_R - h_A)/S_m$ and $2J_{PR}/N = (h_P - h_R)/S_P$, which come from the $\Delta_{RA}(J_{RA}) = 0$ and $\Delta_{PR}(J_{PR}) = 0$, respectively. Simple manipulations of the argument yield the last line above. Taking the thermodynamic limit, $S_m \rightarrow N\Delta M/2$, but $S_P/N \rightarrow 0$, hence $S_P/S_m \rightarrow 0$ in the thermodynamic limit, giving

$$\Pr(0 < J_{PR} < J_{RA}) = \Pr(h_R < h_P < h_R) = 0,$$

as the probability distribution is continuous. Hence, in the thermodynamic limit there is zero probability that $J_{PR} < J_{RA}$. Hence, the value of the coupling required to cause the runaway avalanche to absorb the aftershock following it will always be smaller than the value of the coupling required to cause the precursor to absorb the runaway avalanche, and thus on every sweep of the system it is the aftershock which is absorbed into the runaway avalanche, not the precursor.²⁵

Because it is always an aftershock that is absorbed as $N \rightarrow \infty$, the distribution of jump sizes is identical to the distribution of aftershock avalanche sizes, which is⁴

$$P(S) \sim S^{-\tau} e^{-St^2/2}, \quad (8)$$

where $\tau = 3/2$ and $t = 2J\rho(h_0) - 1$, with h_0 the random local field of the spin which triggers the avalanche. At the critical point $J = J_c$, $t = 0$ and the distribution is a power law, $S^{-\tau}$, as expected at a continuous phase transition.

The parameter t must be evaluated at the local field at which the aftershock to be absorbed begins. We now determine what the local field of the aftershock is. As $N \rightarrow \infty$, $S_m \rightarrow N\Delta M/2$. The value of J is tuned such that $2J/N = (h^* - h_{end})/S_m$, or $h_{end} = h^* - J\Delta M$ for $N \rightarrow \infty$, where h_{end} is the local field of the last spin in the avalanche. This determines the field of the last spin in the runaway avalanche in terms of the field of the first spin in the runaway avalanche, h^* , the current value of the coupling and the fraction of spins in the runaway avalanche, $\Delta M/2$. The fraction $\Delta M/2$ is determined implicitly by

$$\frac{\Delta M}{2} = \int_{h^* - J\Delta M}^{h^*} dh \rho(h). \quad (9)$$

Using the fact that $\rho(h)$ is Gaussian, we may write

this integral in terms of error functions, $\text{erf}(x) = 2/\sqrt{\pi} \int_0^x dt \exp(-t^2)$. We have

$$\begin{aligned}
\Delta M &= \text{erf}\left(\sqrt{\ln(1+j)}\right) \\
&- \text{erf}\left(\sqrt{\ln(1+j)} - \frac{\sqrt{\pi}}{2}(1+j)\Delta M\right), \quad (10)
\end{aligned}$$

where we define $j = J/J_c - 1$ for convenience. For $j = 0$ ($J = J_c$) the unique solution is $\Delta M = 0$. We thus expect that for small j (J close to J_c) ΔM will be small, so we expand the right hand side for small $j > 0$ and ΔM (going to third order in ΔM , as the zeroth order vanishes and the first order cancels with the left hand side). We find

$$\Delta M \simeq \frac{6}{\sqrt{\pi}} j^{1/2}. \quad (11)$$

To lowest order in j , $h^* \simeq 2J_c j^{1/2}/\sqrt{\pi}$,⁴ hence we find $h_{end} \simeq -4J_c j^{1/2}/\sqrt{\pi}$. Now that we have h_{end} we need only determine how far away the next spin is. In the thermodynamic limit the distance between spins tends to zero (as can be shown using the theory of order statistics.²⁶) Hence, h_{end} will only be an infinitesimal distance from the field which begins the following aftershock, so we may evaluate t by inserting $h_0 \simeq h_{end}$. We find $t \simeq -3j$, and so

$$P(S) \sim S^{-\tau} \mathcal{D}(S^\sigma j), \quad (12)$$

with $\tau = 3/2$, $\sigma = 1/2$ and

$$\mathcal{D}(x) = \exp\left[-(ax)^{1/\sigma}/2\right], \quad (13)$$

where $a = 3$. While the parameter a is a non-universal quantity, $\mathcal{D}(x)$ is a universal scaling function and prediction for experiments.

IV. NUMERICAL RESULTS

We test our prediction numerically by simulating the mean field model for many different configurations of spins. We set $R = 1$ in our simulations. Thus, all spins are drawn from a standard normal distribution in our simulations. We can turn the considerations at the beginning of the previous section into an algorithm to compute the jumps in S_m as a function of J . Some caution must be taken, however, as for a finite number of spins the processes PP/AA and PR will necessarily occur on occasion and contribute to jumps in S_m . Eq. (12) is valid only for RA processes in the thermodynamic limit, while the simulations have finite size effects. In order to compare the results of our simulations to the theoretical results, we record only jumps that occur due to RA processes, because that is the dominant process in the thermodynamic limit. Failing to remove the other pro-

N	10^5	10^6	∞
τ	1.48(7)	1.50(6)	1.5
σ	0.50(3)	0.50(7)	1.5
J_c	1.244(3)	1.251(2)	1.253314
a	2.3(2)	2.8(3)	3

TABLE I: Comparison of data collapses, such as in Fig. 4, for numbers of spins $N = 10^5$ and 10^6 . We find the critical exponents τ and σ have the theoretical values within statistical error, and we obtain values for J_c and a , defined in Eq. (13), that are close to the theoretical values, and improve as N is increased. Parentheses indicate estimate error in last digit.

cesses distorts the histograms, resulting in bumps in the histograms at large S .

We ran simulations for 2000 configurations of both 10^4 and 10^5 spins and 400 configurations of 10^6 spins. Fig. (4) shows the results of the 10^6 run. The values of the critical exponents σ and τ are essentially indistinguishable from the theoretical values, with only the values of the non-universal quantities J_c and a (the coefficient of x in Eq. (13), predicted to be 3) being smaller than theoretically predicted. These deviations from the theoretical results are expected to be due to finite size effects, as the values for both J_c and a increase toward the predicted values as N is increased. Table I compares the data for the two different values of N , revealing that as N increases the agreement between theory and simulation improves. Results for $N = 10^4$ are not given, as the data collapse was not satisfactory. However, this data is used in the finite size collapse, discussed below.

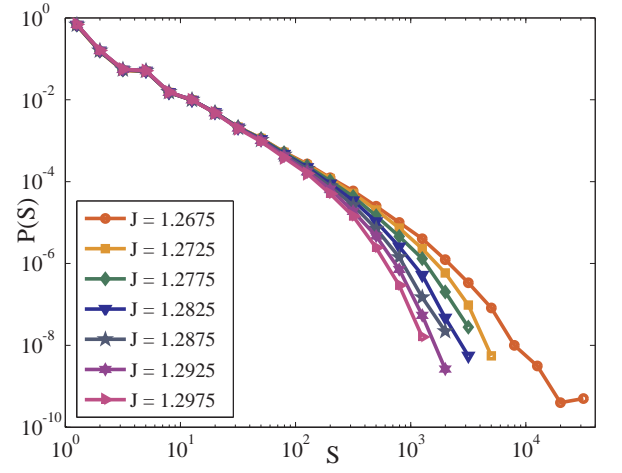
A. Finite Size Scaling Collapse

We also performed a finite-size scaling collapse to determine the critical exponents. By performing a data collapse using the number of spins as a tunable variable we can extract the value of the exponents and J_c in the thermodynamic limit, free of finite-size errors. This method is particularly useful for the analysis of experimental data. For a system of linear size L , we expect the scaling function of Eq. (12) to also depend on L/ξ , where ξ is the correlation length. For the infinite system $\xi \sim j^{-\nu}$; for a finite system ξ cannot exceed the linear system size L , and there are subdominant corrections that are negligible as the number of spins (and hence system size) grows large. We may write

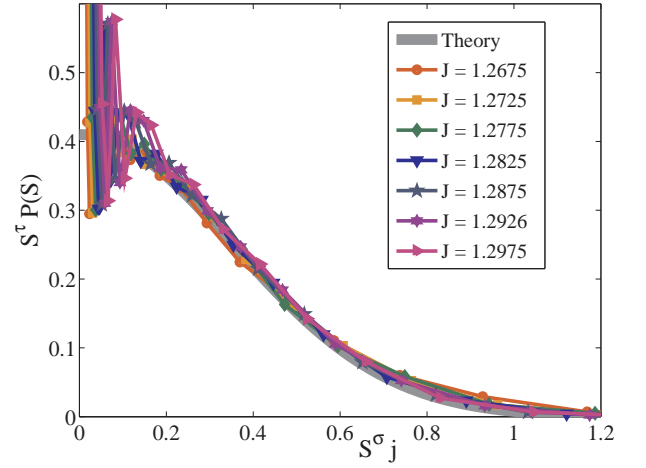
$$P(S) \sim S^{-\tau} \mathcal{D}(S^\sigma j, L^{1/\nu} j),$$

If we now calculate the n^{th} moments of the jump sizes in S_m , $\langle S^n \rangle = \int dS S^n P(S)$, we find:

$$\langle S^n \rangle \sim L^{(n+1-\tau)/(\sigma\nu)} \mathcal{G}(L^{1/\nu} j), \quad (14)$$



(a) Histogram of jump size S for various values of J .



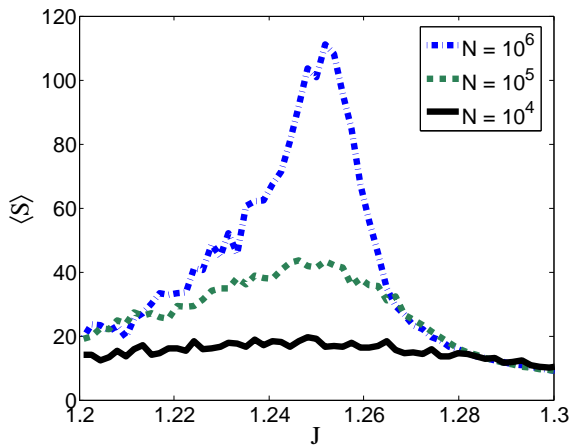
(b) Collapsed Data.

FIG. 4: (Color online) Simulation data. Fig. 4(a) (loglog scale) shows the normalized histograms for different values of J up to about 4% above the critical point. Fig. 4(b) (linear scale) is a collapse of the data, confirming the theoretical values of the universal quantities $\tau = 1.5$ and $\sigma = 0.5$, as well as giving estimates for the non-universal quantities, a and J_c , which are not far off from the predicted values. The discrepancy is due to finite size effects. Note that the data collapse falls almost completely on top of the scaling function, Eq. (13), confirming the scaling form, except near small S , where the scaling form does not apply and discreteness effects become visible.

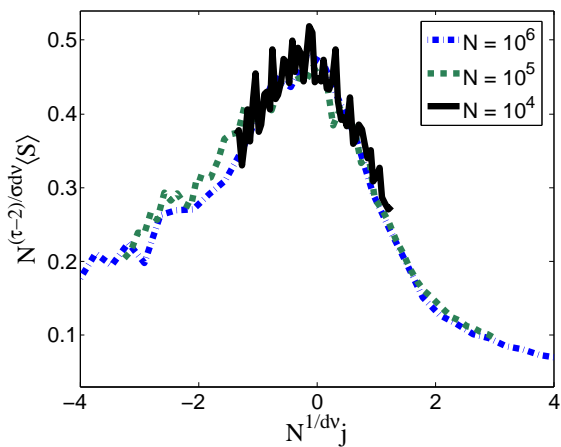
where \mathcal{G} is a new scaling function that depends only on $L^{1/\nu} j$. Using the fact that $N \sim L^d$ for a d -dimensional lattice we obtain

$$\langle S^n \rangle \sim N^{(n+1-\tau)/(\sigma d \nu)} \mathcal{G}(N^{1/(d\nu)} j). \quad (15)$$

In the mean field problem we assume d is effectively the upper critical dimension, d_c , above which mean field theory is exact. The critical dimension is $d_c = 6$ for the RFIM.⁴ As d and ν only appear as $d\nu$, in a scal-



(a)



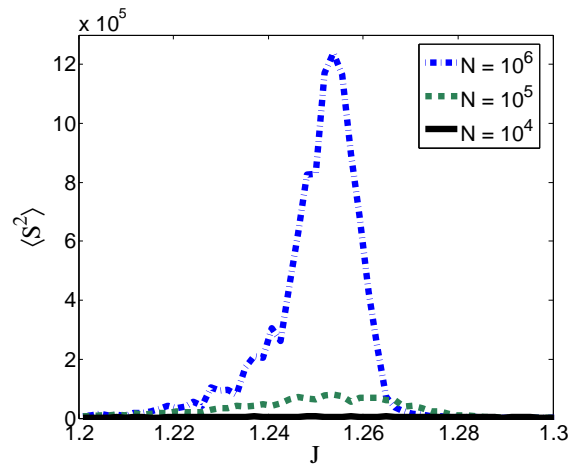
(b)

FIG. 5: (Color Online) (a): $\langle S \rangle$ vs. J . (b): Finite-size scaling collapse. The $N = 10^4$ data appears noisy, but the general trend follows the 10^5 and 10^6 curves.

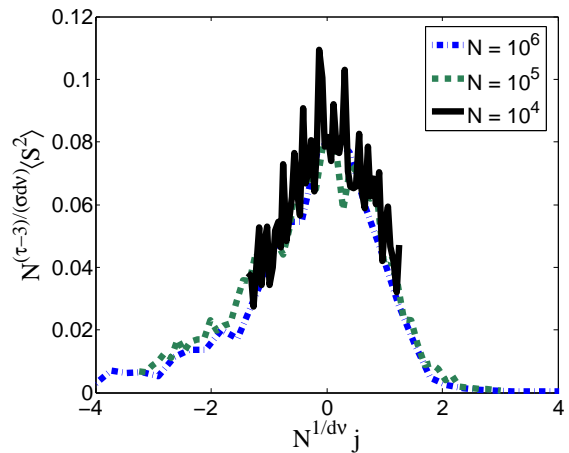
ing collapse (as shown in Figs. (5) and Figs. (6)) we can only determine this combination from the collapse. We calculate $\langle S^n \rangle$ for $n = 1, 2$, and for system sizes of $N = 10^4, 10^5$ & 10^6 . This allows us to determine the exponents $d\nu$ and $(n+1-\tau)/\sigma$, from which we calculate τ , σ , and ν , assuming we may set $d = d_c = 6$ for mean field theory. The results of the collapse are given in Table II. Figs. (5) and Figs. (6) show plots of $\langle S \rangle$ and $\langle S^2 \rangle$, respectively, versus J , with their associated collapses.

V. AVALANCHES IN THREE DIMENSIONS

The physical picture suggested by studying the mean field theory is that the runaway avalanche absorbs aftershock avalanches as J is increased. We expect this to be true in finite dimensions as well. Although the simulations of Ref. 27 find correlations between avalanche sizes



(a)



(b)

FIG. 6: (Color online) (a): $\langle S^2 \rangle$ vs. J . (b): Finite-size scaling collapse. The $N = 10^4$ data appears noisy, but the general trend follows the 10^5 and 10^6 curves.

and waiting times between avalanches at the 3D critical point, which could in principle affect scaling relations, no correlations appear to exist between avalanche sizes. As our arguments do not depend on the time between avalanches, we thus expect the distribution of changes in the runaway avalanche size will be equal to the distribution of aftershock sizes even in finite dimensions. The distribution of aftershock sizes in three dimensions has the same form as Eq. (12) with different values for the exponents τ and σ and a different scaling form $\mathcal{D}(x)$. In three dimensions the exponents are $\tau = 1.6 \pm 0.6$, $\sigma = 0.24 \pm 0.02$ and $\nu = 1.4 \pm 0.2$.⁶ We summarize the derived results for mean field theory and three dimensions in Table III.

n	1	2
$d\nu$	2.6(6)	2.6(5)
$(n+1-\tau)/\sigma$	1.04(22)	3.2(4)
J_c	1.253(2)	1.2529(8)
Derived Exponents	Collapse	Theory
τ	1.5(2)	1.5
σ	0.5(3)	0.5
$d\nu$	2.6(6)	3
ν	0.4(1)	0.5

TABLE II: Results of the finite-size scaling collapse shown in Figs. (5) and Figs. (6) of the n^{th} moments, $\langle S^n \rangle$, of $P(S)$ for $n = 1, 2$. The top table lists the combined exponent values obtained directly from the collapse. The lower table lists the individual exponents determined from these values. We assume $d_c = 6$, giving the estimate $\nu = 2.6/6 \approx 0.4$. The critical exponents are found to be quite close to the expected exponents. Statistical errors in the last digit reported are given in parentheses.

	τ	σ	ν
Mean Field Theory	1.5	0.5	0.5
Three Dimensions	1.60(6)	0.24(2)	1.4(2)

TABLE III: Critical exponents τ , σ and ν in mean field theory and three dimensions. The results for mean field theory are those derived in this work. Those for three dimensions are argued to be the same exponents as those of the aftershock size distribution in three dimensions, reported in Ref. 6. The exponents were determined numerically. Statistical errors in the last digit are given in parentheses.

VI. DIPOLAR INTERACTIONS

We now briefly consider the effect of dipolar interactions between spins. Dipolar forces can give rise to demagnetizing fields which resist the propagation of large avalanches.²⁸ Most magnetization changes in the system are no longer due to nucleation of new domains, but due to motion of domain walls.²⁸⁻³⁰ As a result, the runaway avalanche is broken up into many small avalanches with size distribution $S^{-\tau'} f(S(k/R)^{1/\sigma'})$, with different critical exponents τ' and σ' , and where k is the value of the effective demagnetizing field and $f(x)$ is a universal scaling function.²⁹⁻³¹ Over a large range of H , where the magnetization curve $M(H)$ has constant slope ($dM/dH = \text{constant}$) and is far from saturation, and for disorders R less than some critical disorder R_c^{dipolar} ,³³ the avalanche size distribution only depends on the ratio k/R and does not depend on H ^{29,30}. This is quite different from the case analyzed above, and our previous results do not apply. However, it is interesting for the analysis of experiments on $\text{LiHo}_x\text{Y}_{1-x}\text{F}_4$ and related materials. In these systems the disorder R can be tuned by tuning a transverse magnetic field applied to the sample. Thus, it

may be possible to measure avalanches caused by tuning R using Barkhausen noise²⁰ or other techniques. Domain wall motion can be characterized by an equation of motion^{29,30}

$$\frac{du_i(t)}{dt} = H + \sum_j K_{ij}(u_j - u_i) + h_i, \quad (16)$$

where u is the height of the domain wall, K is an interaction kernel which contains the dipolar and exchange interactions, H is the global magnetic field and the h_i are the random local fields. In the $\text{LiHo}_x\text{Y}_{1-x}\text{F}_4$ experiments tuning the transverse magnetic field amounts to tuning all of the h_i by the same factor. Suppose we tune R until a single spin flips and triggers an avalanche. Because the avalanche size distribution depends on R only through the ratio k/R (as long as $R < R_c^{\text{dipolar}}$), we expect the size statistics of avalanches triggered by tuning R to be given by the same distribution with a different cutoff that scales as $(k/R)^{-1/\sigma'}$, with $\sigma' = 1$ in three dimensions.^{30,32}

VII. EXPERIMENTAL SYSTEMS

Here we give a list of related experimental systems. (1) As mentioned previously, the strength of the random local fields in $\text{LiHo}_x\text{Y}_{1-x}\text{F}_4$ can be tuned by tuning an external magnetic field transverse to the orientation of the spins. In principle, this could be an excellent system to test the results of this work; however, the presence of dipolar forces in such materials changes the behavior of the system, resulting in domain wall motion, as opposed to domain nucleation. This renders such materials unsuitable for studying runaway avalanches. Although in some cases it is possible to minimize the dipolar forces by choosing a suitable sample geometry, such as a frame or thin wire,^{29,30} the perturbative calculation of Ref. 23, which predicts that $\text{LiHo}_x\text{Y}_{1-x}\text{F}_4$ becomes a dipolar-RFIM when a transverse field is applied, assumes the strength of the random local fields is less than the strength of the typical interactions between spins, suggesting that the strength of the random fields is at most comparable to the dipolar forces in this regime. In these materials, we expect domain wall propagation to dominate the dynamics. The results for this case are summarized in section VI.

(2) It is possible to control the exchange interactions between spin-like states in atoms in optical lattice experiments³⁴. This could allow for interesting experimental investigations of avalanches in RFIM-like systems and related systems modeled by the quantum mechanical transverse field RFIM³⁵⁻³⁷, as the coupling is tuned.

(3) Experiments in systems of superfluid ^4He in Nuclepore show hysteretic and avalanching behavior in the amount of fluid trapped in the volume of the Nuclepore as the chemical potential is adjusted.³⁸⁻⁴⁰ There are some qualitative differences between the hysteresis observed in

these experiments and the RFIM. In particular, in fluid experiments the hysteresis curves are typically asymmetric, and do not seem to exhibit runaway avalanches. However, it may still be the case that the two systems are in the same universality class. A first attempt at a comparison between the statistics of the precursor avalanches in these experiments and in the RFIM has been done in Ref. 38. The authors find that the experimental exponents are not inconsistent with the RFIM, but the error bars are not small enough to definitively conclude whether the universality classes are the same or different. Although the systems studied in Ref.'s 38–40 do not display runaway avalanches, this may be because the distribution of pore diameters is wide. A narrower range of pore diameters may allow for large runaway events⁴¹. Additionally, some models of porous media develop a discontinuous jump in the hysteresis loop at sufficiently high porosity,⁴² providing another possible method to achieve runaway events. The group of Ref.'s 38–40 has also found that the coupling between different pores is mediated by a layer of superfluid helium, suggesting that perhaps the coupling can be tuned by adjusting the thickness of the fluid layer. However, the fluid layer thickness does change as the chemical potential is tuned,⁴¹ which may require modification of the results presented in this paper. If runaway avalanches can be triggered in superfluid ⁴He in Nuclepore systems, then it may be possible to study changes in the runaway avalanche size as the coupling between pores is tuned, and the results could be compared to the predictions for the RFIM presented in this work, perhaps with some modifications to account for the coupling changing as the chemical potential is tuned.

(4) The RFIM is applicable to a broad range of systems², ranging from magnets to decision making processes. We expect the results of this paper to be relevant to future studies of many of these systems if the coupling can be tuned.

VIII. CONCLUSION

In summary, we have presented predictions for experiments which study the statistics of changes in the size of a runaway avalanche in a disordered system as the coupling between constituents is tuned. To generate

experimentally testable predictions we have used the random field Ising model to derive the distribution of the size-changes in the runaway avalanche as the ratio J/R is slightly increased above a critical value $(J/R)_c$. We predict the values of the critical exponents in both mean field theory and three dimensions. The exponents found in mean field theory are likely to be those measured experimentally in systems with long range ferromagnetic interactions. For systems with short range interactions, simulations and a renormalization group calculation predict quantitatively accurate values for the exponents.⁴ We argue that in finite dimensions the exponents of the jump in the runaway avalanche size will be equal to the exponents of the aftershock size distribution, which are already known.⁶ Numerical simulations support our theoretical findings. We suggest possibilities for measuring these effects experimentally in ferromagnetic or fluid systems. Further studies could look at finite size effects in the system, such as how events due to processes PR or PP/AA affect the distribution of jump sizes S ,⁴³ or the relation of the RFIM to other systems which exhibit runaway avalanches.

Acknowledgments

We acknowledge NSF grant DMR 10-05209. BAWB gratefully acknowledges a Drickamer Research Fellowship for the University of Illinois. This work was supported by the University of Illinois at Urbana-Champaign. The authors gratefully acknowledge the use of the Turing cluster maintained and operated by the Computational Science and Engineering Program at the University of Illinois. Turing is a 1536-processor Apple G5 X-serve cluster devoted to high performance computing in engineering and science. We thank Yang Liu for writing the Mathematica script which we used to perform the scaling collapses presented in this work, and Nir Friedman, Paul Goldbart, Robert Hallock, David Mertens, Tom Rosenbaum, Moshe Schechter, James Sethna, Georgios Tsekis, Richard Weaver and Stefano Zapperi for helpful conversations. We thank our anonymous referees for helpful comments which improved the discussion in the paper. B.A.W.B. would like to thank Barry Brinkman for helpful feedback on this manuscript.

-
- ¹ J. P. Sethna, K. A. Dahmen, & C. R. Myers, *Nature* **410**, 242 (2001).
 - ² J. P. Sethna *et al.*, *Phys. Rev. Lett.* **70**, 3347 (1993).
 - ³ K. A. Dahmen & J. P. Sethna, *Phys. Rev. Lett.* **71**, 3222 (1993).
 - ⁴ K. Dahmen & J. P. Sethna, *Phys. Rev. B* **53**, 14872 (1996).
 - ⁵ O. Perkovic, K. Dahmen, & J. P. Sethna, *Phys. Rev. Lett.* **75**, 4528 (1995).
 - ⁶ O. Perkovic, K. A. Dahmen, & J. P. Sethna, *Phys. Rev. B* **59**, 6106 (1999).

- ⁷ E. Vives *et al.*, *Phys. Rev. Lett.* **72**, 1694 (1994).
- ⁸ M. C. Kuntz *et al.*, *Comp. Sci. Eng.* **1**, 73 (1999).
- ⁹ R. da Silva & M. Kardar, *Phys. Rev. E* **59**, 1355 (1999).
- ¹⁰ J. Villain, *Phys. Rev. Lett.* **52**, 1543 (1984).
- ¹¹ P. Shukla, *Phys. Rev. E* **62** 4725 (2000).
- ¹² M. J. Alava *et al.*, *Phys. Rev. B* **71**, 064423 (2005).
- ¹³ Dj. Spasojevic, S. Janicevic, & M. Knezevic, *Europhys. Lett.* **76**, 912 (2006).
- ¹⁴ M. Muller & A. Silva, *Phys. Rev. Lett.* **96**, 117202 (2006).
- ¹⁵ Y. Liu & K. A. Dahmen, *Phys. Rev. E* **76**, 031106 (2007).

- ¹⁶ Y. Liu & K. A. Dahmen, Phys. Rev. E. **79**, 061124 (2009).
- ¹⁷ G. Grinstein & J. F. Fernandez, Phys. Rev. B. **29**, 6389 (1984).
- ¹⁸ D. S. Fisher, Phys. Rev. Lett. **56**, 416 (1986).
- ¹⁹ A. J. Bray & M. A. Moore, J. Phys. C: Solid State Phys. **18**, L927 (1985).
- ²⁰ H. Barkhausen, Phys. Z. **20**, 401 (1919).
- ²¹ J. Marcos *et al.*, Phys. Rev. B. **67**, 224406 (2003).
- ²² A. Berger, A. Inomata, J. S. Jiang, J. E. Pearson, S. D. Bader, & K. Dahmen, J. Appl. Phys. **89**, 7466 (2001).
- ²³ M. Schechter, Phys. Rev. B. **77**, 020401(R) (2008).
- ²⁴ D. M. Silevitch, G. Aeppli & T. F. Rosenbaum, Proc. Nat. Acad. Sci., **107**, 2797 (2010).
- ²⁵ Unless, of course, it were to happen that all of the after-shock avalanches were absorbed, in which case PR events would contribute to changes in S_m as there would be no more RA events. This can happen in finite systems for large J/R .
- ²⁶ S. S. Wilks, Bull. Amer. Math. Soc. **54**, 6 (1948).
- ²⁷ B. Cerruti & E. Vives, Phys. Rev. E. **80**, 011105 (2009).
- ²⁸ M. C. Kuntz & J. P. Sethna, Phys. Rev. B. **62**, 11699 (2000).
- ²⁹ P. Cizeau, S. Zapperi, G. Durin & H. E. Stanley, Phys. Rev. Lett. **79**, 4669 (1997).
- ³⁰ S. Zapperi, P. Cizeau, G. Durin & H. E. Stanley, Phys. Rev. B. **58**, 6353 (1998).
- ³¹ G. Durin & S. Zapperi, Phys. Rev. Lett. **84**, 4705 (2000).
- ³² S. Zapperi, Private communication (2011).
- ³³ H. Ji & M. O. Robbins, Phys. Rev. B. **46**, 14519 (1992).
- ³⁴ L.-M. Duan, E. Demler & M. D. Lukin, Phys. Rev. Lett. **91**, 090402 (2003).
- ³⁵ T. Senthil, Phys. Rev. B. **57**, 8375 (1998).
- ³⁶ A. Dutta, B. K. Chakrabarti & R. B. Stinchcombe, J. Phys. A: Math Gen. **29**, 5285 (1996).
- ³⁷ K. Ghosh & J. K. Bhattacharjee, Phys. Lett. A **238**, 203 (1998).
- ³⁸ M. P. Lilly & R. B. Hallock, Phys. Rev. B. **64**, 024516 (2001).
- ³⁹ M. P. Lilly, A. H. Wootters & R. B. Hallock, Phys. Rev. B. **65**, 104503 (2002).
- ⁴⁰ M. P. Lilly, A. H. Wootters & R. B. Hallock, Phys. Rev. Lett. **77**, 4222 (1996); A. H. Wootters & R. B. Hallock, Phys. Rev. Lett. **91**, 165301 (2003).
- ⁴¹ R. B. Hallock, Private communication (2011).
- ⁴² M. L. Rosinberg, E. Kierlik & G. Tarjus, Europhys. Letters **62**, 377 (2003); See also: F. Detcheverry, E. Kierlik, M. L. Rosinberg & G. Tarjus, Phys. Rev. E. **68**, 061504 (2003); F. Detcheverry, E. Kierlik, M. L. Rosinberg & G. Tarjus, Phys. Rev. E. **72**, 051506 (2005).
- ⁴³ We have some results on this, which demonstrate that as J grows large the distribution has a sharp decay followed by a small rebound which peaks quickly and then decays again. This occurs in a finite system when all aftershocks have been absorbed by the runaway avalanche and the system starts to absorb PR events.